Sensors & Diagnostics

PAPER

View Article Online
View Journal | View Issue

Cite this: *Sens. Diagn.*, 2025, **4**, 407

Selective sensing of heavy metal ions using carbon dots synthesized from *Azadirachta indica* seeds†

Somedutta Maity,[b] Santhosh Kumar,[b] Gurmeet Singh,[a] Sukanya Patra,[a] Divya Pareek[a] and Pradip Paik *[a]

There have been notable advancements in the technology associated with using waste resources to create novel and beneficial products. This study demonstrates that the kernel part of *Azadirachta indica* (Neem) seeds can be sustainably used for this purpose. Carbon dots (CDs) of approximately *ca.* 4–8 nm in size were synthesized from the kernel *Azadirachta indica* seeds through calcination, followed by surface modification using diethylamine, sodium methoxide, and alcohol. This produced waste seed-derived luminous surface-quaternized CDs (Ai-CDs). These CDs were used as a fluorescent nanoprobe to detect inorganic contaminants at concentrations ranging from low (5 μM) to high (120 μM), due to their strong photostability and excitation-dependent emission in aqueous solutions. Ai-CDs were used to measure the levels of Cd^{+2} and As^{3+} in solution through quenching of luminescence intensity ("turn-off"), while cupric ions (Cu^{+2}) selectively increased fluorescence ("turn-on") for sensing. The current method of synthesising CDs offers quick reaction times, along with great selectivity and sensitivity. The CDs preferentially absorbed Cd^{2+} and As^{3+}, causing a sharp dimming in fluorescence intensity by 27% and 30%, respectively. In contrast, for Cu^{+2} and Cu^{+} the fluorescence intensity was enhanced. Consequently, this unique characteristic was utilized to exclude and identify Al^{3+}, Cd^{2+}, Mn^{2+}, Ni^{2+}, Co^{2+}, Cu^{2+}, and Cu^{+} ions, with detection limits ranging from 5 μM to 120 μM. Furthermore, we demonstrated the heavy metal ion sensing activity of CDs from their salt solutions, highlighting their potential as environmentally friendly metal ion detection agents. A cell viability assay was carried out, revealing that the CDs are non-toxic.

Received 17th November 2024,
Accepted 18th February 2025

DOI: 10.1039/d4sd00350k

rsc.li/sensors

1. Introduction

Nowadays, heavy metal ions pose a serious issue, particularly in rapidly developing countries.[1] Recently, there has been a lot of focus on the need for highly effective methods to identify heavy metals. Cadmium (Cd^{2+}) and arsenic ions (As^{+3}) are two main concerns due to their high toxicity. Heavy metal ions threaten the environment and ecological balance due to their toxicity.[2] Consequently, identifying heavy metal ions has become a major focus for researchers.[3]

Heavy metals, defined by having an atomic weight greater than 20 and a density[4] greater than 5.0 g cm^{-3}, were initially believed to be naturally occurring and non-threatening to human health and ecology.[1] Due to the recent industrial revolution, the levels of heavy metals increased in rivers, lakes, and soils. Cd(II) is one of the most hazardous heavy metal ions, polluting soil and water primarily through industrial waste, and subsequently entering the food chain, directly or indirectly.[5] Bioaccumulation of heavy metals in the human body can cause various acute illnesses, including dysfunction of the neurological and digestive systems, renal failure, bone weakness, degeneration of testicular tissues and red blood cells, and even genetic abnormalities.[6] Once heavy metals accumulate in water sources or living organisms, they enter the food chain, leading to their presence in the human body.[7] As soon as heavy metal ions enter the body, they interact with enzymes and proteins without being metabolized,[8] resulting in the loss of biological activity. Continued accumulation of heavy metal ions can cause acute kidney failure (AKD),[9] memory loss,[10] breathing difficulties,[11] and potentially cancer.[12]

The US Environmental Protection Agency (USEPA) stipulates that the highest permissible concentration of heavy metals in drinking water should be less than 1.3 ppm for Cu, 2 ppb for Hg, 15 ppb for Pb, 10 ppb for As, 5 ppb for Cd, and 100 ppb for Cr.[13] Given these concerns, the detection and elimination of heavy metal ions are essential. Extensive research has been conducted on unconventional methods for removing Cd(II) from

[a] *School of Biomedical Engineering, Indian Institute of Technology (BHU), Varanasi 221 005, UP, India. E-mail: paik.bme@iitbhu.ac.in, pradip.paik@gmail.com*
[b] *School of Engineering Sciences and Technology, University of Hyderabad, Hyderabad 500 046, Telangana, India*

† Electronic supplementary information (ESI) available. See DOI: https://doi.org/10.1039/d4sd00350k

water, particularly through adsorption, due to its simplicity, cost-effectiveness, and diversity of adsorbent material and renewal options.[14] Nanomaterials can potentially remove heavy metals, specifically Cd(II), from water. Carbon-based nanomaterials, specifically carbon nanotubes (CNTs) and carbon dot (CDs) composites, have garnered a lot of attention due to functional groups containing oxygen on CDs, such as epoxy, carbonyl groups on the basal plane, and carboxylic groups on the edges.[15,16] In the last few years, there has been a growing interest in the identification and detection of the process of fluorescence quenching, which is a process whereby quantum yield decreases in fluorescence due to various molecular interactions with quencher molecules. There are several methods available for the detection of heavy metal ions, including ICP emission spectroscopy, fluorescence spectroscopy, UV-visible spectroscopy, and atomic absorption.[17] Among these, fluorescence spectroscopy stands out as an appealing technique for heavy metal detection due to its precise sensitivity, facile operation, and broad detection range.

To address specific concerns, numerous modifications to CDs utilizing other materials have been investigated. A notable problem in the detection of heavy metal ions is their tendency to reduce emissions, resulting in intense fluorescence quenching. Quenching refers to the process in which the fluorescence intensity of a given substance decreases, typically due to excited-state reactions. Given their high specific surface area and abundant reactive sites for heavy metals, CDs have attracted substantial attention from researchers for heavy metal detection. As a result, carbon nanoparticles serve as ideal candidates for heavy metal detection. Additionally, CDs are advantageous for wastewater treatment due to their availability, low cost, and antibacterial properties.[18] Furthermore, CDs functionalized with hydroxyl groups enhance the detection of heavy metal ions in effluents.

This research focuses on heavy metal detection using carbon quantum dots (Ai-CDs) synthesized from *Azadirachta indica* seeds through a solid-state synthesis method. It is necessary to assess the presence of hazardous components in the Ai-CDs, such as and Cd. The concentrations of heavy metal elements are typically at the μg mL^{-1} level, with fluorescence quenching and ICP-MS analysis conducted to determine their amounts. Heavy metal ions can form charge transfer complexes, where the fluorescence emitted by the Ai-CDs is quenched by energy transfer from the metal's lowest excited singlet state to another electronic state, resulting in fluorescence loss. The interaction between the two light-sensitive components–Ai-CDs as the donor and heavy metal ions as the acceptor–causes dynamic quenching. ICP-MS provides the benefits of high sensitivity and simultaneous multielement analytical capacity. This study assesses the ICP-MS's ability to quantify the amounts of both healthy elements and heavy metals present in Ai-CDs, detecting several heavy metals, including lower concentrations of As(III) and Cd(II). Finally, the biocompatibility of Ai-CDs was confirmed through the MTT assay, demonstrating that they are not toxic to cells and can effectively detect analytes in the physiological media.

2. Experimental

2.1. Materials and reagents

Unprocessed *Azadirachta indica* seeds were collected from the farmhouse of the institute, washed, dried, and stored on a hot plate at 60 °C for 24 h. The chemicals required for synthesizing carbon dots, *i.e.*, sodium methoxide (CH_3ONa) (98%, SRL), diethyl amine [$(CH_3–CH_2)_2NH$] (99%, SRL), and methanol (CH_3OH) (99.5%, SRL), were used without further purification. Ultrapure water was used for all experiments. Detailed synthesis methods have been filed for Indian patents (ref no: 202111060434, dated: 23rd December 2022).

2.2. Synthesis of carbon dots

Ai-CDs were produced using a solid-state reaction procedure. A tube furnace was used to directly heat a crucible containing 1.0 g of neem seed kernel to 400 °C (Ai-CDs-1) and 450 °C (Ai-CDs-2) while maintaining a constant argon flow at a rate of 5 °C min^{-1} for two hours. After cooling to room temperature, the resulting black-brown powder was dissolved in clean water. Next, diethyl amine, sodium methoxide, and methanol were used to modify the surface to create luminous surface-quaternized CDs (Ai-CDs). The solid-phase approach produced Ai-CDs with an 83% yield. It is notable that detailed synthesis methods have been filed for Indian patents (ref no: 202111060434, dated: 23rd December 2022).

2.3. Characterization

TEM studies were conducted using a FEI Technai G2S-Twin TEM equipped with a 200 kV acceleration voltage. Solid-state X-ray powder diffraction (XRD) experiments were carried out using a Bruker D8 Advance diffractometer with non-monochromatic Cu Kα X-ray radiation. A PerkinElmer LS 55 spectrofluorometer was used for photoluminescence (PL) investigations. UV-vis spectroscopy experiments were conducted in the 180–900 nm range (model: Lambda 750 spectrometer, PerkinElmer). Solid samples were analyzed using Raman spectroscopy (model: WITech Alpha 300 Raman spectrometer). Thermal stability was investigated using a thermogravimetric analyzer (TGA) in an N_2 environment from 30 °C to 1000 °C at a heating rate of 10 °C min^{-1}. FTIR (Nicolet model Impact-410) was used to identify the chemical functionality of the Ai-CDs. Several heavy metals, along with lower amounts of elements, such as 'As' and 'Cd', were detected using ICP-MS (Agilent 7800). Sample preparation was the most important phase in the analytical investigations and needed thorough examination to minimize errors. For our sample preparation, we used 2% HNO_3 for 24 h for the digestion of unwanted components. Solid samples were once again studied using Raman spectroscopy (WITech Alpha 300 Raman spectrometer).

To calculate quantum yields (QY), a CD solution with a maximum absorption of 0.1 at the absorption maxima was prepared. The solution was set to an excitation wavelength (λ = 270–310 nm), and the emission spectra were subsequently

acquired. The absorbance spectra were collected on an Eppendorf bio-spectrophotometer, and fluorescence spectra were measured using a Hitachi spectrofluorometer (model no. F 7000). The relative quantum yield was calculated according to the literature,[19] assuming a quantum yield (QY) of 0.34% for the coumarin standard.[20]

2.4. Metal quenching studies

The main focus of this work was to determine the effect of various parameters on the ability to absorb and remove heavy metals, specifically Cd(II) ions and As(III). Metals can produce charge transfer complexes with CDs. The molecule should fluoresce is quenched by energy transfer from the metal's lowest excited singlet state to another electronic state, resulting in a loss of fluorescence. The interaction between two light-sensitive molecules–a donor and an acceptor–causes dynamic quenching. The donor fluorophore transfers energy to the acceptor, which may then emit light or absorb the energy entirely. Electron excitation occurs prior to the quenching phase in dynamic quenching.

2.5. Cytotoxicity test

To assess the cytotoxicity of Ai-CDs, an MTT assay was performed using normal splenocytes. Normally, 104 cells/150 mL of spleen cells were cultivated in a 96-well plate for 24 h at 37 °C in a humidified incubator with 5% CO_2. Afterward, 100 mL of Dulbecco's modified Eagle's medium (DMEM) with different doses of Ai-CDs (0, 20, 50, 100, 200, and 500 mg mL^{-1}) was added and incubated for an additional two hours. The supernatant was removed, and the spleen cells were gently washed in a PBS solution. After adding 150 mL of DMEM and incubating for 4 h, 20 mL of the MTT solution (5 mg mL^{-1}) was added. The culture media containing MTT was then removed, and 150 mL of DMSO was added to the mixture, which was shaken for 10 min at room temperature (25 °C). Spleen cell-free versions of the same trials served as controls. Finally, an enzyme-linked immunometric meter was used to measure the average optical density (OD) at 490 nm. Cell viability was determined using the formula:[21]

$$\text{Cell viability} = \text{OD sample/OD control}$$

A similar experiment was followed to assess the cytotoxicity of MDA-MB-231 cells with different concentrations of CDs, and cellular morphology was examined after 24 h of incubation under the MTT assay using optical microscopy.

3. Results

Seeds of the *Azadirachta indica* kernel served as the only carbon source for synthesizing Ai-CDs using a calcination process, as shown in Scheme 1. The calcination temperature and heating duration are crucial for the formation of Ai-CDs. The two reaction parameters were optimized to increase the quantum yield and emission wavelength of Ai-CDs. The

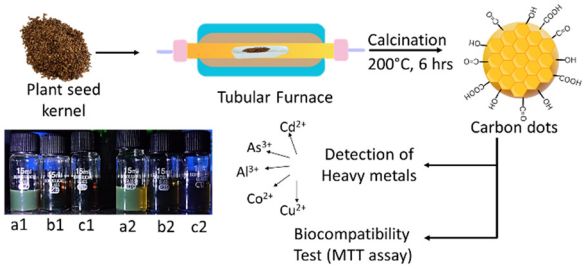

Scheme 1 The synthesis approach of CDs from the kernel part of *Azadirachta indica*. Emission obtained from Ai-CDs-1 treated with: za1) only CDs (untreated), b1) with Cd^{2+}, and c1) with As^{3+}. Emission obtained from Ai-CDs-2 treated with: a2) only CDs (untreated), b2) with Cd^{2+}, and c2) with As^{3+}.

carbon core of Ai-CDs generates fluorescence due to the presence of surface functional groups and defects. Additionally, an appropriate calcination period is essential for producing high-performance Ai-CDs. As a result, 400 °C and 2 h of calcination time were selected as the optimal parameters, with the resultant Ai-CDs exhibiting red emission and a high quantum yield. The morphology and size distribution of Ai-CDs were characterized through HRTEM (-Fig. 1b–d). As shown in Fig. 1(a–d), the obtained Ai-CDs are monodispersed and exhibit no aggregation. Their particle sizes range from 4–8 nm, with an average diameter of ~6 nm for (Ai-CDs-1) and 7 nm for (Ai-CDs-2). Fig. 1b and d show the HRTEM images of Ai-CDs-1 and Ai-CDs-2, respectively, exhibiting fringes indicative of the crystalline nature of CDs. The hydrodynamic diameter of Ai-CDs-1 was found to be 13.56 nm, while that of Ai-CDs-2 was 19.78 nm (Fig. 1e). Notably, the hydrodynamic diameter of the solvent is greater than the size of Ai-CDs obtained from HRTEM due to the high surface zeta potential (ζ) that interacts with water molecules. The zeta potential analysis was carried out to quantify the charges on the surface of CDs and assess their colloidal stability. Ai-CDs have ζ values of −35.12 mV for Ai-CDs-1 and −33.72 mV for Ai-CDs −2 (Fig. 1f), indicating the presence of hydroxyl (–OH) and carboxyl (–COOH) functional groups. This high ζ value provides the CDs with more colloidal stability.

The FTIR analysis helps ascertain the chemical functionalities attached to the surface of Ai-CDs. The FTIR spectrum of the kernel part of neem seeds and the as-prepared Ai-CDs is shown in Fig. 2. The characteristic bands of functional groups for Ai-CDs-1 appear at 3305 cm^{-1} (N–H/O–H, stretch), 1729 cm^{-1} (C═O, stretch), 1434 cm^{-1} (H–O, bending), 1063 cm^{-1} (O–C, stretch), and 871–837 cm^{-1} (C–H, bending) (Fig. 2a). For Ai-CDs-2, the bands are at 3021 cm^{-1} (C–H), 2933 (C–H, stretching), 2848 cm^{-1} (N–H, stretching), 1557 cm^{-1} (N–O, stretching), 1422 cm^{-1} (O–H, bending), 1218 cm^{-1} (O–H, stretching), 750 cm^{-1} (C–H, bending), and 669 cm^{-1} (C═C, bending) (Fig. 2b).

The BET adsorption–desorption isotherms of Ai-CDs indicate a type-IV isotherm with a hysteresis loop (Fig. 2c and d), representing the porous structure of the CDs. The degassing

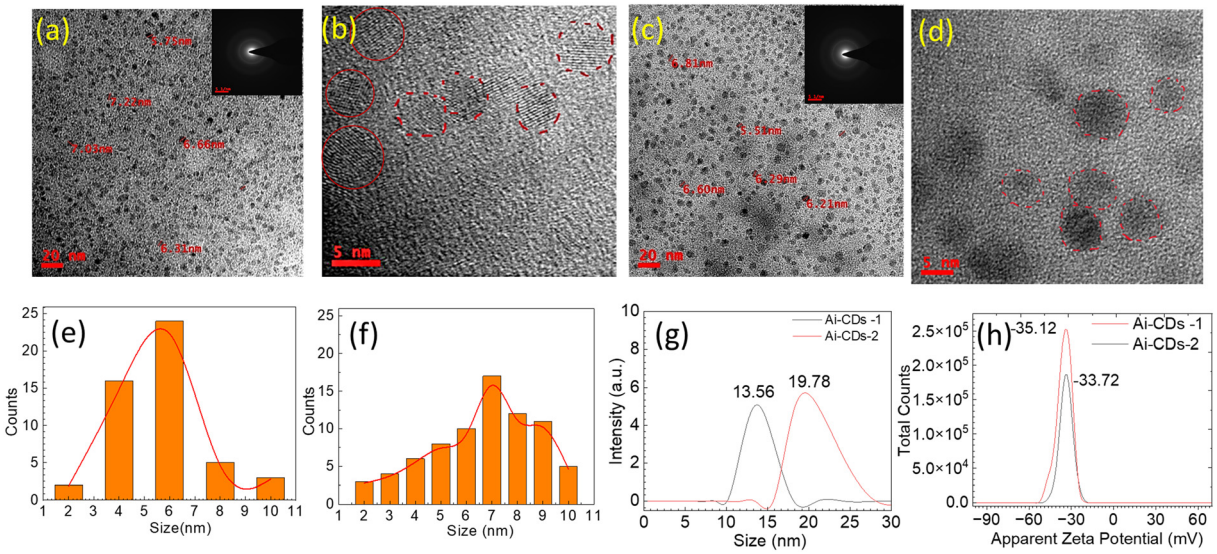

Fig. 1 (a and b) TEM images of Ai-CDs-1 at lower and higher magnifications, respectively and (c and d) TEM images of Ai-CDs-2 at low and high magnifications, respectively. The inset of Fig. (a) shows the SAED pattern of Ai-CDs-1, and the inset of Fig. (c) shows the SAED pattern of Ai-CDs-2, (e and f) size distribution of Ai-CDs-1 and Ai-CDs-2 respectively obtained from TEM images considering 500 particles, Fig. (g) particle size distribution for the Ai-CDs-1 and Ai-CDs-2 measured through DLS in a water medium, and Fig. (h) the zeta potential profiles for Ai-CDs-1 and Ai-CDs-2 measured in the water medium to exhibit highly negative surface zeta potential and colloidal stability.

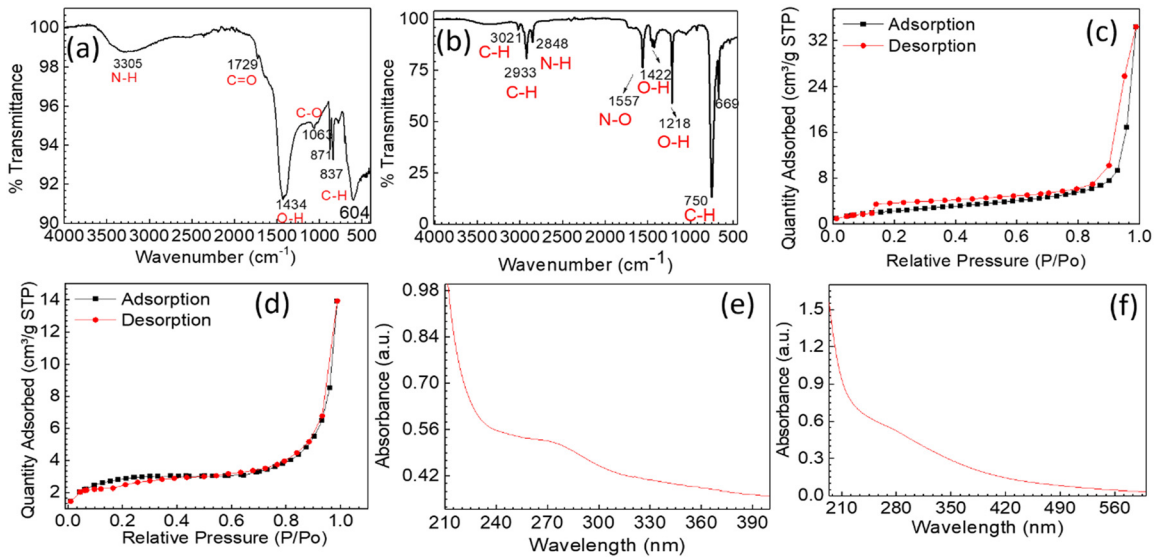

Fig. 2 (a and b) FTIR spectra of Ai-CDs-1 and Ai-CDs-2, (c and d) BET N_2-adsorption–desorption isotherms for Ai-CDs-1 and Ai-CDs -2, (e and f) UV-vis spectra for Ai-CDs-1 and Ai-CDs-2, respectively.

process was performed at 150 °C for 4 h. The BET surface area of Ai-CDs-1 was calculated to be 9.6862 $m^2\ g^{-1}$, whereas Ai-CDs-2 yielded 8.7338 $m^2\ g^{-1}$. The high surface area of the CDs, along with their chemical functionalities, facilitates interactions with metal ions, enhancing their fluorescence quenching performance.

The ocular image of CDs dispersed in water (Fig. S1†) and absorbance measured in the presence of UV light for Ai-CDs-1 and Ai-CDs-2 is shown in Fig. 2(e and f). The synthesized CDs, when suspended in water, exhibit significant emission under UV radiation (at 273 nm and 268 nm). The UV-vis absorption spectrum of the as-synthesized CDs is shown in Fig. 2(e and f), with absorption bands related to C=C bonds and the n–π* transition of C=O bonds.

Fig. 3a displays the powder XRD patterns of Ai-CDs-1 and Ai-CDs-1. The XRD pattern indicates the crystalline nature of the CDs. The sharp peaks are attributed to this crystalline nature, as confirmed by the SAED pattern of HRTEM (Fig. 1c and e). From Fig. 3a, it can be concluded that the diffraction peaks appear at 2θ = 22–28°, 41°, 50°, and 60° due

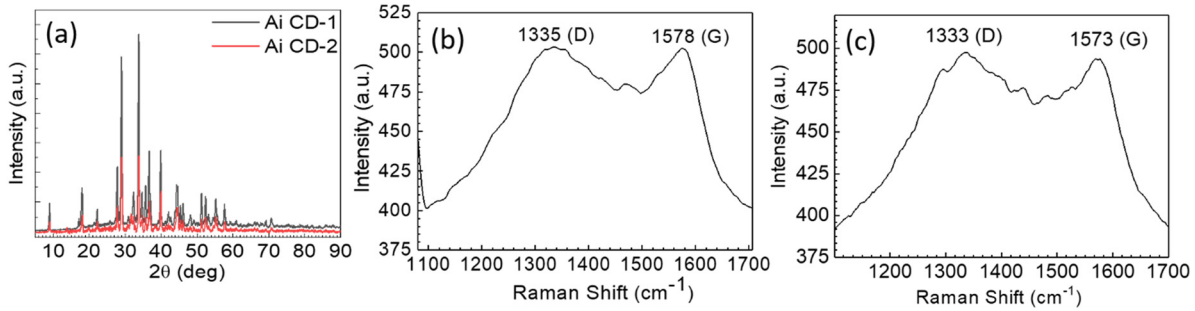

Fig. 3 (a) The XRD pattern of synthesized carbon dots Ai-CDs-1 and Ai-CDs-2, and (b and c) Raman spectroscopic analysis of Ai-CDs-1 and Ai-CDs-2, respectively.

to the (002), (100), (102), and (103) diffraction planes.[22] The thermal stability of CDs is confirmed through TGA (Fig. S2†). The weight loss of Ai-CDs-1 is found to be ~20% at 40–150 °C due to moisture loss. In the temperature range of 151–620 °C, mass loss is attributed to the decomposition of organic components present in the CDs, while there is almost no weight loss beyond 720 °C. Ai-CDs-2 shows a 20% weight loss around 40–130 °C, followed by weight loss ranges of 130–390 °C and around 580 °C due to the decompositions of carbon residuals. TGA for both Ai-CDs-1 and Ai-CDs-2 is shown in Fig. S2.† DSC for both samples confirms exothermic peaks due to decomposition (Fig. S3†). The Raman spectroscopic analysis of the solid-state structure of the CDs has been performed. Fig. 3(b) and (c) present the typical Raman spectra of Ai-CDs-1 and Ai-CDs-2, respectively, highlighting two distinct bands corresponding to the D and G bands. The D band is located at 1333 cm^{-1} for Ai-CDs-1 and at 1335 cm^{-1} for Ai-CDs-2, indicating the presence of disordered sp^2-hybridized carbon atoms. Conversely, the G band is located at 1573 cm^{-1} and at 1578 cm^{-1} for Ai-CDs-1 and Ai-CDs-2, respectively, corresponding to in-plane stretching vibrations (E_{2g}) of crystalline graphite carbon atoms. The graphitization degrees for Ai-CDs-1 and Ai-CDs-2 were found to be 0.847 and 0.846, respectively.

Furthermore, the quantum yields (QY) of the CD samples were calculated. As discussed in the methodology section, CD solutions with a maximum absorption of 0.1 at their absorption maxima were prepared. Solutions of CDs with absorption maxima were set to an excitation wavelength (λ = 270–310 nm), and the emission spectra were subsequently acquired. The relative QY was calculated according to the reported literature,[19] assuming the QY of the coumarin standard as 0.34%.[20] Quantum yields of Ai-CDs-1 and Ai-CDs-2 were determined to be 4.20% and 3.03%, respectively.

3.1. Fluorescence spectroscopy studies of Ai-CDs for heavy metal detection

Previous reports on CDs have highlighted their non-toxic and hydrophilic characteristics for fluorescence sensing. Consequently, the newly designed facile synthesis approach, using attractive sustainable carbon sources has prompted researchers to focus on CDs. This synthesis method can significantly reduce production costs and make large-scale production feasible. However, the fluorescence quenching properties of the CDs change when they react with metal ions due to the presence of surface functional groups on the CDs. Typically, a suitable plane of a CD sensor can optically detect heavy metals (metal ions).[23] The selection of a carbon source is critical, and the synthesis of the CDs is a primary condition. In optical sensing, the interaction between CDs and metal ions can alter the dot's optical signal, resulting in a decrease or change in the intensity of emission or absorption spectra.[24] All solutions were prepared in double-distilled water immediately before performing the quenching assay. Concentrated CD dispersion was sonicated and used to produce 3 mL of solutions. Fluorescence measurements of CD samples were carried out with increasing concentrations of 0, 10, 20, 40, 60, 80, and 120 μM of metal ions (Al^{3+}, Cd^{2+}, Mn^{2+}, Ni^{2+}, Co^{+2}, Cu^{2+}, Cu^{+}, and As^{+3}). Prior to spectroscopic experiments, the samples were stirred using a magnetic stirrer for approximately 20 s (RPM 300), following the addition of metal ion solutions. From these experiments, we observed that the fluorescent intensity of the CDs changed when the metal ions were added gradually compared to the absence of heavy metal ions. Broadly, the surface oxygen moieties on CDs, responsible for coordinating with metal ions, are effective colorimetric and fluorometric detectors. The acquired camera image of AI-CDs-1 treated with: a1) only CDs (untreated), b1) with Cd^{2+}, and c1) with As^{3+}; AI-CDs-2 treated with a2) only CDs, b2) with Cd^{2+} and c2) with As^{3+} is shown in the supporting file (Fig. S1†). It is evident that the fluorescent signal changes with the treatment of heavy metal ions.

These results indicate the specific interaction between metal ions and CDs. If a metal ion does not affect the fluorescent signal of CDs, it cannot be utilized as a fluorescence signal. As a result, we assessed the detection system's selectivity by capturing fluorescence spectra in the presence of several metal ions (Scheme 2). One of the key characteristics examined was fluorescence properties. As a result, we evaluated the fluorescence intensity quenching or enhancing effects of various metal ions on Ai-CDs in deionized water (Fig. 4 and 5). The influence of metal ions (*e.g.*, Al^{3+}, Cd^{2+}, Mn^{2+}, Ni^{2+}, Co^{2+}, Cu^{2+},

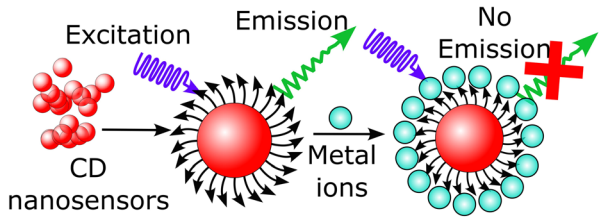

Scheme 2 A diagrammatic representation of the heavy metal ion-CDs nano sensor quenching process.

Cu^{+}, and As^{+3}) is significant for pollution and health hazards. The fluorescent intensity of CD solutions was measured in the presence of various metals. We investigated the metal-induced fluorescence using Al^{3+}, Cd^{2+}, Mn^{2+}, Ni^{2+}, Co^{2+}, Cu^{2+}, Cu^{+}, and As^{3+} metal ion solutions. Compared to the emissions of Al^{3+}, Cd^{2+}, Mn^{2+}, Ni^{2+}, Co^{+2}, and As^{+3}, the fluorescence emission was significantly reduced, while Cu^{2+} and Cu^{+} showed a notable enhancement of fluorescence[25] (Fig. 4 and 5).

Notably, the fluorescence responses of our Ai-CDs in the presence of various metal ions, such as Al^{3+}, Cd^{2+}, Mn^{2+}, Ni^{2+}, Co^{+2}, Cu^{2+}, Cu^{+}, and As^{+3}, at concentrations of (top to bottom) 0, 10, 20, 40, 60, 80, and 120 μM, were measured. The decrease in the intensity of fluorescence spectra for Al^{3+}, Cd^{2+}, Mn^{2+}, Ni^{2+}, Co^{+2}, and As^{+3} is illustrated with the percentage decrease in fluorescence intensity as the concentration of the metal ions increases. Furthermore, the fluorescence quenching effects of Cd^{2+} (−30%) and As^{+3} (27%) Ai-CDs-1 (Fig. 6a) are significantly higher than those of other ions, such as Al^{3+}, Mn^{2+}, Ni^{2+}, and Co^{+2}. Additionally, we examined the detection capabilities of Cu^{2+} and Cu^{+} using CDs. Our CDs exhibited an increase in fluorescence emission when Cu^{2+} or Cu^{+} were added to the solution, with intensity rising in proportion to the concentrations of these ions. The metal ion quenching capacities for Ai-CDs-2 (Fig. 6b) resemble those of Ai-CDs-1 (Fig. 6a); however, the intensity varies depending on the concentrations of various metal ions, such as Cd^{2+} (29.7%) and As^{+3} (27.7%). This fluorescence amplification is caused by the affinity of the functional groups for Cu^{2+} and Cu^{+} ions. The fluorescence emission of CDs in the presence of copper at varying concentrations, such as from top to bottom: 0, 10, 20, 40, 60, 80, 120, and 140 μM, respectively, is displayed in Fig. 6a and b. The presence of Cd^{2+} and As^{+3} metal ions on the CD surface was detected using ICP-MS (see table in Fig. 6).

The effect of Ai-CDs on cell proliferation was examined using the MTT assay to assess the biocompatibility of Ai-CDs *in vitro* on normal splenocytes (Fig. 7a and b) and MDA-MB-231 cells (Fig. 7c). To study whether CDs affect cell proliferation, the MTT assay (Fig. 7) was performed for Ai-CDs-1 and Ai-CDs-2. Cells were treated with concentrations of 0, 15.62, 31.25, 62.5, 12.5, 250, 500, and 1000 μg mL^{-1} for 24 h. After 24 h of CD treatment, normal cells showed over 90% viability at concentrations of 125 μM and 250 μM. These results indicate that CDs are biocompatible up to 125 μM and 250 μM for 24 h of incubation. Fig. 8 presents microscopy images showing the morphology of the cells after the MTT assay performed at 125 μg mL^{-1}. It is evident that there is no change in the morphology of the cells after incubation with different concentrations of CDs.

4. Conclusions

In the past few decades, numerous studies on carbon dots have been reported, predominantly focusing on their applications in

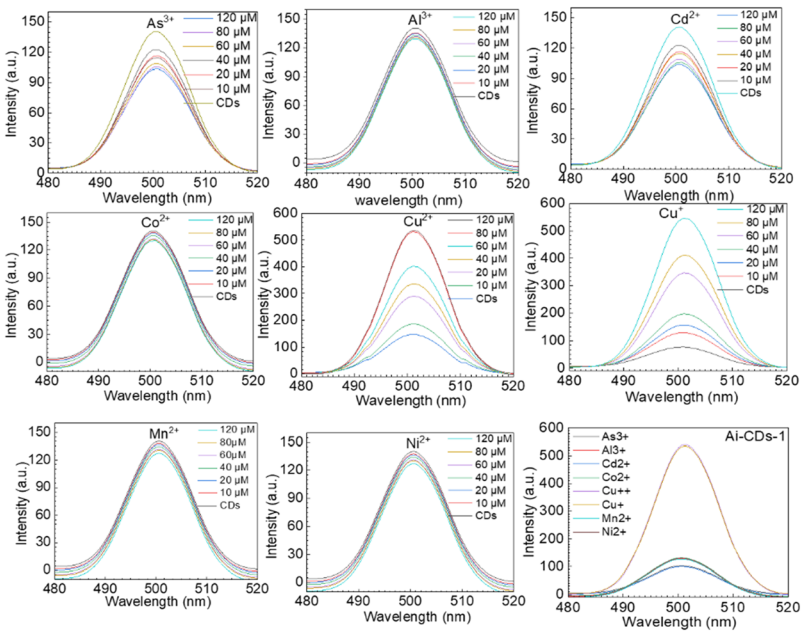

Fig. 4 Fluorescence spectra of Ai-CDs-1 with different concentrations of metal ions, such as Al^{3+}, Cd^{2+}, Mn^{2+}, Ni^{2+}, Co^{+2}, Cu^{2+}, Cu^{+}, and As^{+3}, at different concentrations, such as 0, 10, 20, 40, 60, 80, and 120 μM.

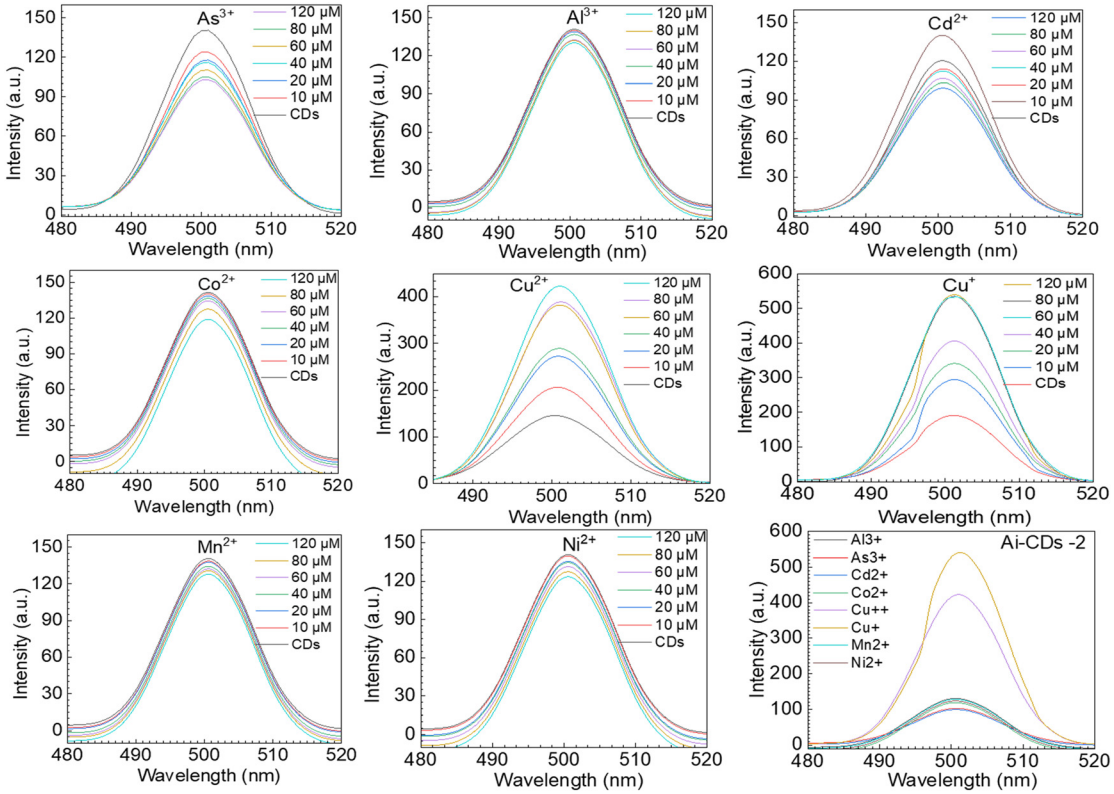

Fig. 5 Fluorescence spectra of Ai-CDs-2 with different concentrations of metal ions, such as Al^{3+}, Cd^{2+}, Mn^{2+}, Ni^{2+}, Co^{+2}, Cu^{2+}, Cu^{+}, and As^{+3}, at concentrations of 0, 10, 20, 40, 60, 80, and 120 μM.

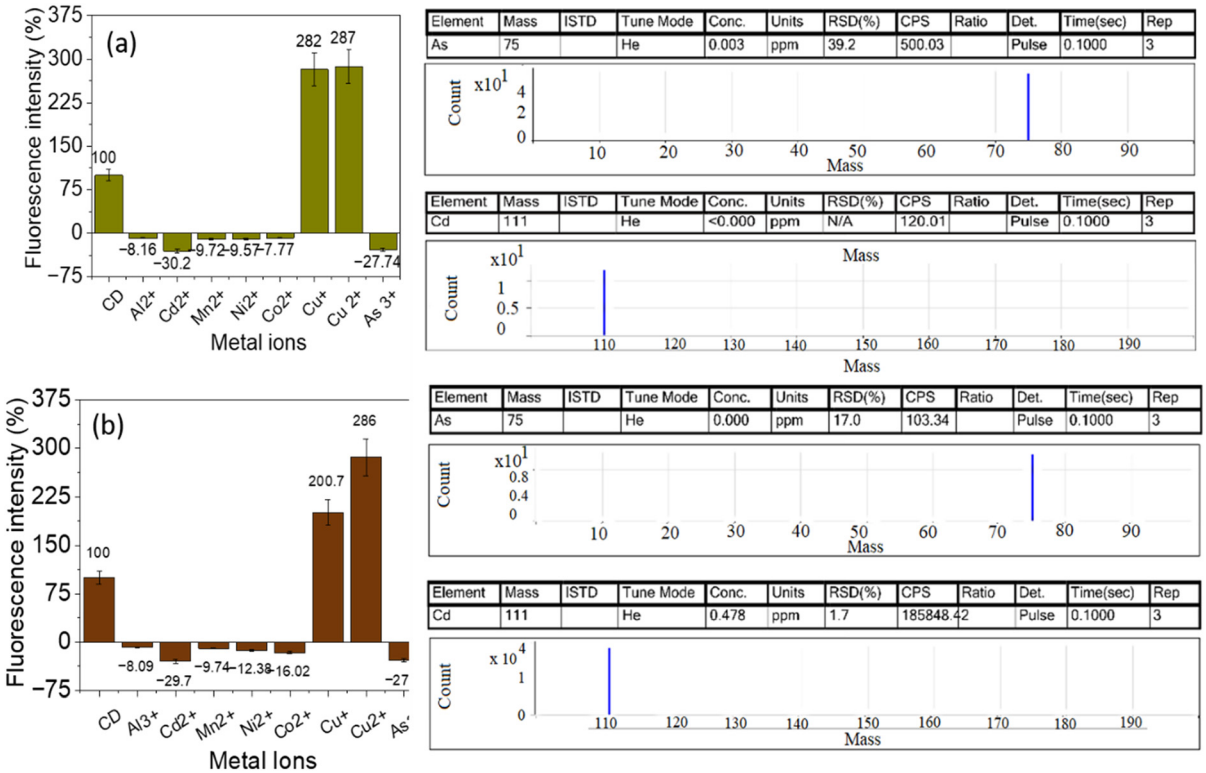

Fig. 6 (a and b) Fluorescence intensity percentage ratios $(F–F_0)/F_0$ for Ai-CDs-1 and Ai-CDs-2 with different ions (Al^{3+}, Cd^{2+}, Mn^{2+}, Ni^{2+}, Co^{+2}, Cu^{2+}, Cu^{+}, and As^{+3}), along with ICP-MS data for As^{+3} and Cd^{2+} ions on the surface of CDs.

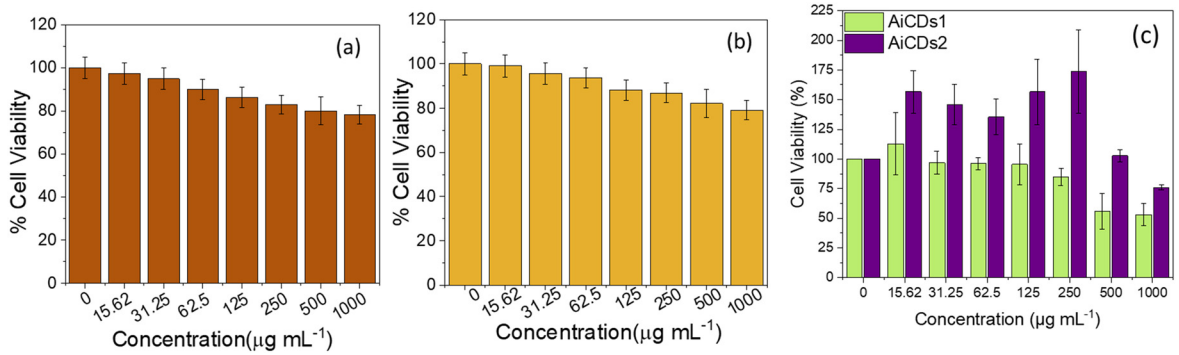

Fig. 7 Cell viability (%) as assessed by MTT assay performed with varying concentrations of (a) AI-CDs-1 and (b) AI-CDs-2 at different concentrations (0, 15. 62, 31. 25, 62. 5, 125 250, 500, and 1000 μg mL^{-1}) at 37 °C for 24 h in (a) normal splenocytes. (c) Cell viability (%) was estimated by MTT assay with different concentrations of AI-CDs-1 and AI-CDs-2 using MDA-MB-231 cells.

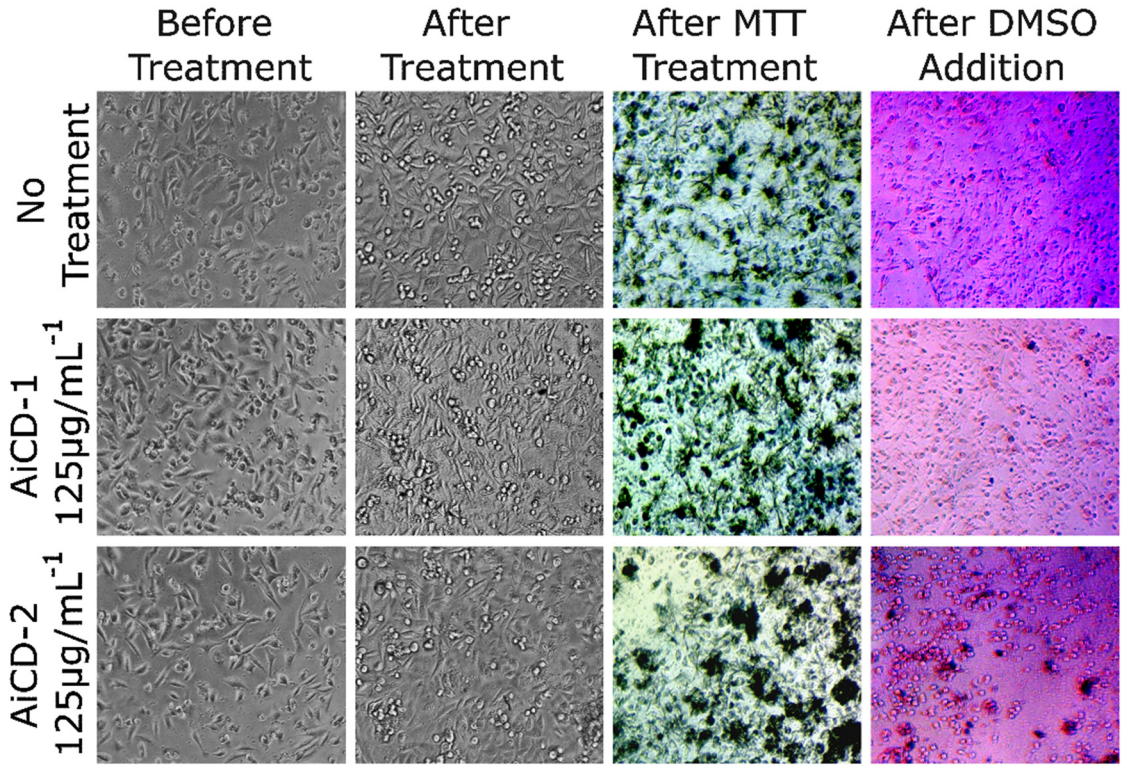

Fig. 8 Representative microscopy images showing the morphology of the cells after the MTT assay performed at 125 μg mL^{-1}. MDA-MB-231 cells were used to acquire the microscopy images.

bio-imaging. Recent developments using the fluorescent properties of CDs have facilitated the creation of portable heavy metal detectors. The results suggest that CDs facilitate the development of heavy metal sensors. Despite various synthetic techniques being reported, the poor water solubility of CDs and the need for low-cost manufacturing of devices remain significant challenges for the application of CDs in many industries. Ai-CDs measured the concentrations of Cd^{2+} and As^{3+} through luminescence quenching, resulting in a "turn-off" effect. In contrast, cupric and cuprous ions uniquely enhance fluorescence, creating a "turn-on" effect for sensing. This method provides the advantages of rapid reaction times, along with high selectivity and sensitivity. The CDs can effectively absorb Cd^{2+} and As^{3+}, resulting in a significant dimming of fluorescence. Our study demonstrates that the sensitivity of Ai-CDs in detecting heavy metal ions can be as low as 10 μM. Ai-CDs synthesized using a green synthesis process are biocompatible. The synthesized Ai-CDs are spherical with diameters of 6–7 nm, emitting light, while quantum yields for Ai-CDs-1 and Ai-CDs-2 were found to be 4.20% and 3.03%, respectively. These CDs are capable of detecting metal ions, such as Al^{3+}, Mn^{2+}, Ni^{2+}, Co^{+2}, Cu^{2+}, Cu^{+}, Cd^{2+}, and As^{+3},

through fluorescence quenching. The detection ability is concentration-dependent. Additionally, this study demonstrates an efficient, environmentally friendly, and straightforward method for detecting heavy metal ions, particularly Cd^{2+} and As^{+3}. However, further clarification is needed regarding the precise mechanisms behind the various photoluminescent effects, which depend on the synthetic process and unprocessed carbon sources. However, carbon-based quantum dots for heavy metal sensing may lead to the development of more economical and environmentally friendly synthetic techniques for various applications.

Data availability

The data that supports the findings of this study are available from the corresponding author upon reasonable request.

Author contributions

P. Paik is the main project investigator (PI). Ideation, experimental design, experimental results analysis, and manuscript writing were performed by Somedutta, Santhosh, and P. Paik. Characterization was assisted by Sukanya, Divya, and Gurmeet. All authors checked and approved the manuscript for publication.

Conflicts of interest

The authors declare no conflicts of interest.

Acknowledgements

The authors acknowledge the financial support awarded to Prof. Paik by the I-DAPT foundation (ref. I-DAPT/IT (BHU)/2023-24/Project Sanction/47), the Indian Council of Medical Research (ICMR), India (Ref: EMDR/SG/12/2023-4724), STARS-IISc., Bangalore (ref. MoE-STARS/STARS-2/2023-0318), and the Anusandhan National Research Foundation (ANRF), India (ref: CRG/2023/005576). Somedutta and Gurmeet Singh acknowledge the financial support (Ph.D. fellowships) from CSIR, India (file no. 9/0013/11053/EMR/I).

References

1 J. Briffa, E. Sinagra and R. Blundell, *Heliyon*, 2020, **6**, e04691.
2 H. Medhi, S. S. Khumukcham, B. Manavathi and P. Paik, *RSC Adv.*, 2020, **10**, 24095–24107.
3 R. Ding, Y. H. Cheong, A. Ahamed and G. Lisak, *Anal. Chem.*, 2021, **93**, 1880–1888.
4 P. B. Tchounwou, C. G. Yedjou, A. K. Patlolla and D. J. Sutton, *Exper. Suppl.*, 2012, **101**, 133–164.
5 N. A. A. Qasem, R. H. Mohammed and D. U. Lawal, *npj Clean Water*, 2021, **4**, 36.
6 S. Kolluru, S. Agarwal, S. Sireesha, I. Sreedhar and S. Kale, *Process Saf. Environ. Prot.*, 2021, **150**, 323–355.
7 M. Balali-Mood, K. Naseri, Z. Tahergorabi, M. R. Khazdair and M. Sadeghi, *Front. Pharmacol.*, 2021, **12**, 643972.
8 J. JAIN and P. GAUBA, *Int. J. Pharma Bio Sci.*, 2020, **82**, 125–150.
9 O. Barbier, G. Jacquillet, M. Tauc, M. Cougnon and P. Poujeol, *Nephron Physiol.*, 2005, **99**, 105–110.
10 K. M. Bakulski, Y. A. Seo, R. C. Hickman, D. Brandt, H. S. Vadari, H. Hu and S. K. Park, *J. Alzheimer's Dis.*, 2020, **76**, 1215–1242.
11 B. Nemery, *Eur. Respir. J.*, 1990, **3**, 202–219.
12 H. S. Kim, Y. J. Kim and Y. R. Seo, *J. Cancer Prev.*, 2015, **20**, 232–240.
13 E. C. Okpara, O. E. Fayemi, O. B. Wojuola, D. C. Onwudiwe and E. E. Ebenso, *RSC Adv.*, 2022, **12**, 26319–26361.
14 A. Biswas, B. P. Chandra and C. Pratibha, *Appl. Surf. Sci.*, 2023, **612**, 155841.
15 X. Yang, Y. Wan, Y. Zheng, F. He, Z. Yu, J. Huang, H. Wang, Y. S. Ok, Y. Jiang and B. Gao, *Chem. Eng. J.*, 2019, **366**, 608–621.
16 S. Perumal, R. Atchudan, P. Thirukumaran, D. H. Yoon, Y. R. Lee and I. W. Cheong, *Chemosphere*, 2022, **286**, 131760.
17 F. M. Shimizu, M. L. Braunger and A. Riul, *Chemosensors*, 2019, **7**, 1–19.
18 H. S. Tohamy, M. El-Sakhawy and S. Kamel, *J. Fluoresc.*, 2023, **33**, 423–435.
19 A. M. Brouwer, *Pure Appl. Chem.*, 2011, **83**, 2213–2228.
20 K. E. Oberhofer, M. Musheghyan, S. Wegscheider, M. Wörle, E. D. Iglev, R. D. Nikolova, R. Kienberger, P. St. Pekov and H. Iglev, *RSC Adv.*, 2020, **10**, 27096–27102.
21 S. Maity, M. S. Tomar, K. Wasnik, S. Patra, M. Das Modak, P. S. Gupta, D. Pareek, M. Singh and P. Paik, *ACS Biomater. Sci. Eng.*, 2022, **8**, 3608–3622.
22 N. Sharma, I. Sharma and M. K. Bera, *J. Fluoresc.*, 2022, **32**, 1039–1049.
23 Y. Zhang, A. Ye, Y. Yao and C. Yao, *Sensors*, 2019, **19**, 247.
24 X. Sun and Y. Lei, *TrAC, Trends Anal. Chem.*, 2017, **89**, 163–180.
25 S. Maity, M. Das Modak, M. S. Tomar, K. Wasnik, P. S. Gupta, S. Patra, D. Pareek, M. Singh, M. Pandey and P. Paik, *Biomed. Mater.*, 2024, **19**, 25043.